

## Sensitive Determination of Lead(II), Copper(II), and Mercury(II) Based on B/P-doped Ordered Mesoporous Carbons

Yu-Long Xie<sup>1,\*</sup>, Fa-Ping Ye<sup>1</sup>, Qian-Ni Guo<sup>1</sup>, He-Lin Ye<sup>2</sup>

<sup>1</sup> Key Laboratory of Resource Chemistry and Eco-environmental Protection in Tibeta Plateau of State Ethnic Affairs Commission, School of Chemistry and Chemical Engineering, Qinghai Nationalities University, Xining, Qinghai, 810007, China

<sup>2</sup> School of Chemistry and Chemical Engineering, Lanzhou City University, Lanzhou 730070, China

\*E-mail: [yulongxie2012@126.com](mailto:yulongxie2012@126.com)

Received: 19 June 2020 / Accepted: 20 September 2020 / Published: 31 October 2020

---

The B/P-doped ordered mesoporous carbons (B/P-doped OMCs) were synthesized as a surface modification of electrode, which has result in some latest developments of electrochemical sensors for detecting heavy metal ions. In this study, boron and phosphorus were co-incorporated into OMCs through a facile aqueous self-assembly using a hydrothermal doping strategy. The structure and its electrochemical performance were studied, the B/P-doped OMCs not only owns the common features of carbon material ,but also demonstrate the advanced eletrochemical detecting capacities on lead(II), copper(II), and mercury(II).

---

**Keywords:** B/P-modified ordered mesoporous carbons, detect, lead(II), copper(II) ; mercury(II)

### 1. INTRODUCTION

The discharge of industrial effluents during recent decades has caused serious environmental pollution owing to the heavy metal ions of industrial wastewater [1,2]. These dangerous metal ions can lead to a potential threat to the safety of the ecological environment and human survival, because it's very difficult to remove them from the water, and easy to accumulate in the body [3,4]. Therefore, we must find effective methods and materials to detect and remove them from the aqueous solutions.

Up to now, a variety of methods have been developed under the circumstances; including membrane separation [5], electrochemical oxidation [6], coagulation/flocculation [7], photocatalysis [8], biological treatment [9]and adsorption [10]. Among them, electrochemical method is considered as one of the most promising and efficient method for the treatment of trace amounts of heavy-metal ions from large volumes of water.

In electrochemical detecting method, which attracts the focus of scientists that the electrode

modified with all kind of films. The modified electrodes can reduce overpotential, improve the sensitivity and reaction rate, and improved selectivity [11]. In electrode materials, the OMC(ordered mesoporous carbons) demonstrated an advantageous performance for sensing heavy metals. In addition to the general nature of high specific surface area arising from all kinds of porous carbon materials, OMCs are further improved with periodically arranged uniform mesopore space, alternative pore shapes, and tunable pore sizes [12-14]. They are exhibiting a fascinating ability for advanced applications in heterogeneous catalysis and energy conversion. Meanwhile, the various applications of OMCs are not only associated with their advantageous physical properties, such as thermal conductivity, electric and mesostructural associated parameters, but also to their chemical reactivities [15].

The intrinsic chemical properties of ordered mesoporous carbons can be easily modified by the heteroatom functionalization on graphene geometries such as at the defects, edges or strained regions [16]. A great deal of research has been carried out in development of heteroatom (such as B, N, O, P, S) incorporated ordered mesoporous carbons as advanced electrode materials in electrochemical energy storage or as an alternative to current catalysts for biomass conversion.

N-doped OMCs with a graphitic wall structure is a good metal-free basic catalyst [17] and catalyst support [18]. Most recently, according to reports, the P-doped porous carbon possessed an improvement in photocurrent generation and a much better electrical conductivity [19], which is advantage for energy storage devices. In order to fully display the potential applications of dual-heteroatom-doped OMCs, at the same time comprehend the roles that the heteroatoms play, the exploration of dual-heteroatom-containing functional groups on OMCs becomes necessary of more scientifically.

In this work, boron/phosphorus-doped OMCs were fabricated through a solvent-evaporation-induced self-assembly, which allows the dual heteroatom incorporated polymer processes a moderate energy density, large power density, and long cyclic stability [20-23]. The as-obtained dual-hetero doped OMCs were with B/P incorporation, extraordinary electrochemical capacitance, and tailorable microstructure. The electrochemical properties of the B/P dual incorporated OMCs were estimated as electrodes of supercapacitors.

## 2. EXPERIMENTAL

### 2.1. Reagents and apparatus

All chemical reagents were of analytically pure grade and were used without any purification. Ultra pure water was obtained from Milli-Q academic. An acetate buffer solution of pH 5.0 was prepared by mixing proper proportions of 0.1 M NaAc and 0.1 M HAc. Ultra pure Milli-Q water was used throughout the work and its resistivity was over 18 M $\Omega$ ·cm.

All electrochemical experiments were performed on a CHI 660E electrochemical workstation at room temperature. A standard three-electrode system was employed to study the electrochemical performances. The three-electrode system with a bare or modified glassy carbon electrode (GCE) as the working electrode. The three-electrode system was employed with a saturated calomel electrode (SCE)

as the reference electrode and a platinum wire as the counter electrode. The morphologies and structures of the samples were characterized by a (JSM-6500, JEOL Ltd., Tokyo, Japan) transmission electron microscopy (TEM). The as-prepared samples were characterized by a powder X-ray diffraction on Rigaku Ultima IV X-ray diffractometer with Cu K $\alpha$  irradiation ( $\lambda=0.15406$  nm).

## 2.2. Synthesis of boron-modified ordered mesoporous carbons

The hydrothermal methods were used in the synthesis of the B- and P-doped mesoporous carbon using resorcinol as the carbon source, and boric acid and phosphoric acid as the heteroatom-doped source to modulate the carbon properties. The PEO-PPO-PEO triblock copolymer F127 was used as the structure directing agent in the self-assembly process. The product can be used in synthesis of resorcinol, boric acid, and phosphoric acid. The synthesis process, a stirred mixture of 2.0 g resorcinol, 0.6 g boric acid, 1.2 g phosphoric acid, and 2.0 g F127 were dissolved in a solution containing 10.0 mL water, and 10.0 mL ethanol under magnetic stirring until the solution became transparent. After that, 2.0 g formaldehyde (37 wt%) and 0.6 g HCl (32 wt%) were added to the solution and stirred for 2 h. Subsequently, the transparent homogeneous mixture was hydrothermally processed at 150 °C for 8 h. The solution separated into two layers, the upper solution was discarded and the interface film peeled off. After that, the rest of the products were dried at 80 °C for 10 h, and then carbonized under an Ar atmosphere at 800 °C for 3.0 h with a heating rate of 5.0 °C $\cdot$ min $^{-1}$ .

## 2.3. Fabrication of the electrochemical sensor

Prior to the modification, a bare GCE was carefully polished to a mirror-like surface using 0.3, and 0.05 mm alumina slurry and sonicated in ultra pure water. After that, the electrode was successive ultrasonic treatment with ethanol and ultra pure water and subsequently dried at room temperature. The B/P-doped OMCs materials were uniformly dispersed in 0.05% Nafion solution via ultrasonic treatment, resulting in a homogeneous black suspension. Then, 5  $\mu$ L of B/P-doped OMCs materials solution was dropped on the pretreated bare GCE and dried at the room temperature.

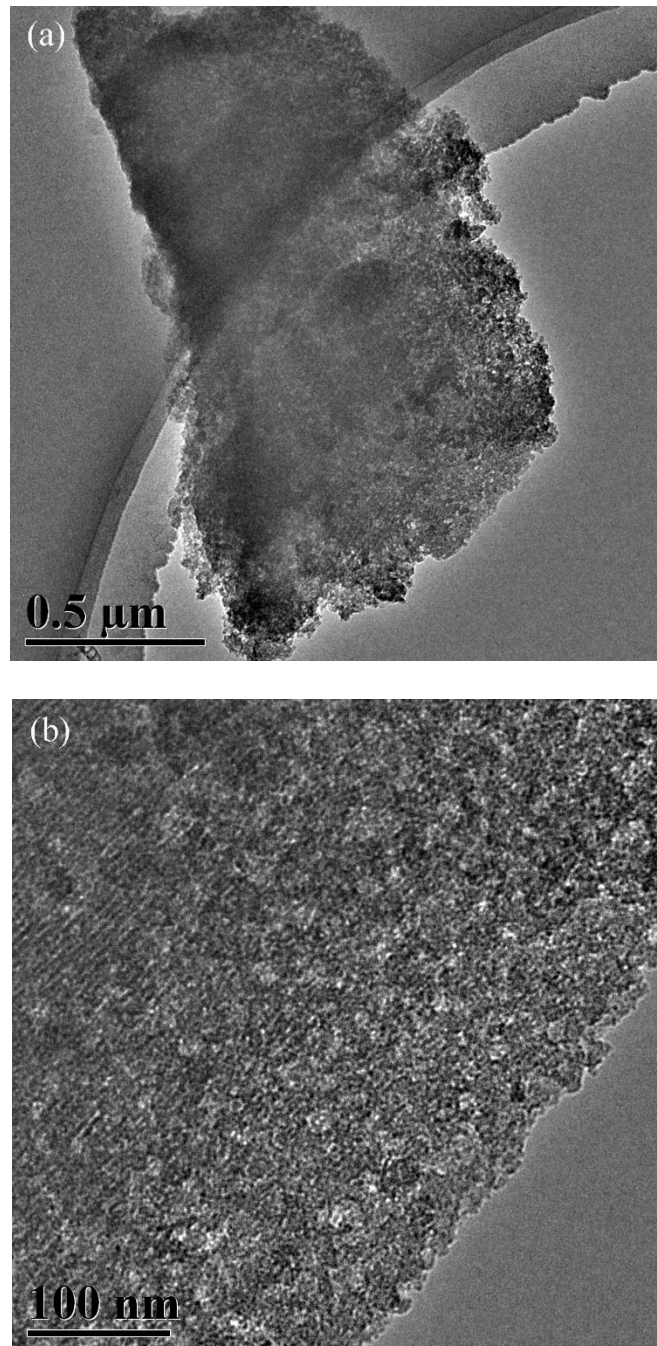
## 2.4. Electrochemical measurements

A differential pulse anodic stripping voltammetric (DPASV) method was used to the sensitive detection of Pb $^{2+}$ , Cu $^{2+}$ , and Hg $^{2+}$  under optimal conditions. The electrochemical scan rate was set at 25 mV $\cdot$ s $^{-1}$  because which presented higher anodic peak currents for Pb $^{2+}$ , Cu $^{2+}$ , and Hg $^{2+}$ . The peak current increased in higher with a pulse amplitude up to 100 mV. Consequently, the optimized parameters of DPASV for simultaneous determination of Pb $^{2+}$ , Cu $^{2+}$ , and Hg $^{2+}$  were potential range of  $-1.0$  to  $+0.6$  V (vs. SCE); scan rate of 25 mV $\cdot$ s $^{-1}$ , 100 mV pulse amplitude.

## 3. RESULTS AND DISCUSSION

The morphology of B/P-doped OMCs was characterized by TEM as displayed in Fig. 1. As seen

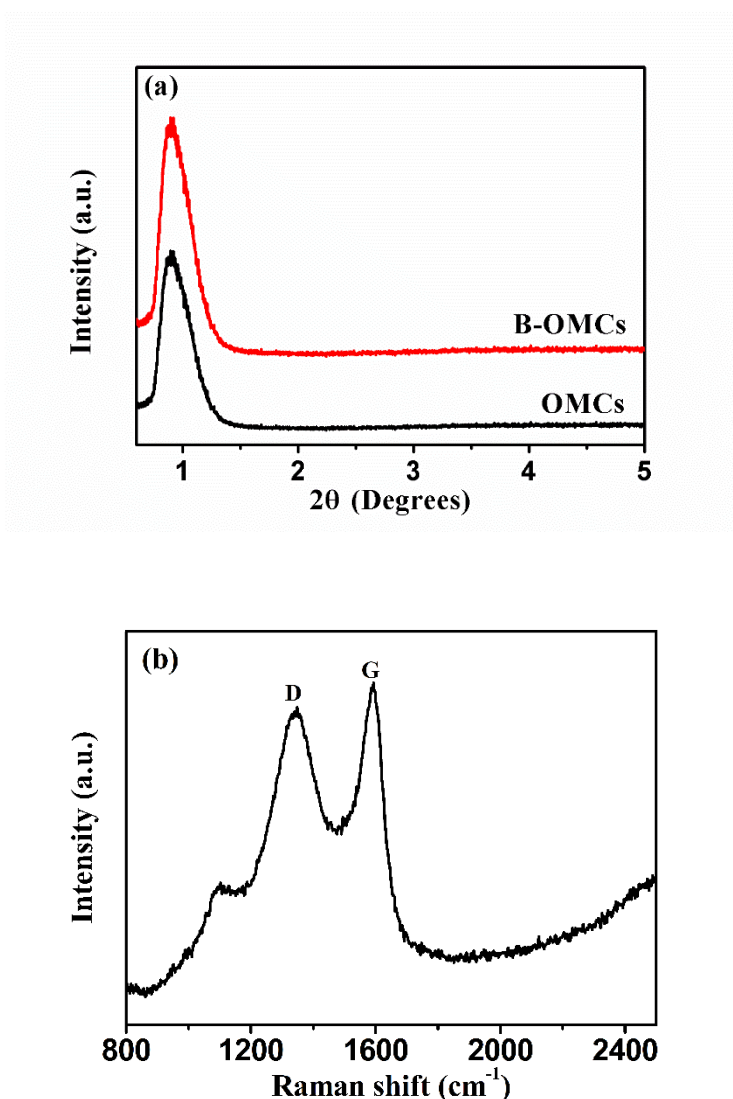
from low-magnification TEM images (Fig. 1a), the B/P-doped OMCs display a certain amount of pore structure. Fig. 1b displays high-magnification TEM images indicating that the B/P-doped OMCs may present well ordered architectures, at the same time, some lattice disorder architectures and structural defects appeared, which may play a significant role in electrolyte ion and charge accommodation region.



**Figure 1.** TEM image of B/P-doped OMCs.

Fig. 2a displays the low-angle XRD patterns of B/P-doped OMCs. The evident diffraction peak is found at around  $2\theta = 1.0^\circ$ , the strong peaks of the B/P-doped OMCs centered at around  $2\theta = 1.0^\circ$  can be indexed as the (100) reflection of ordered 2D hexagonal mesostructures, indicating that the B/P-doped

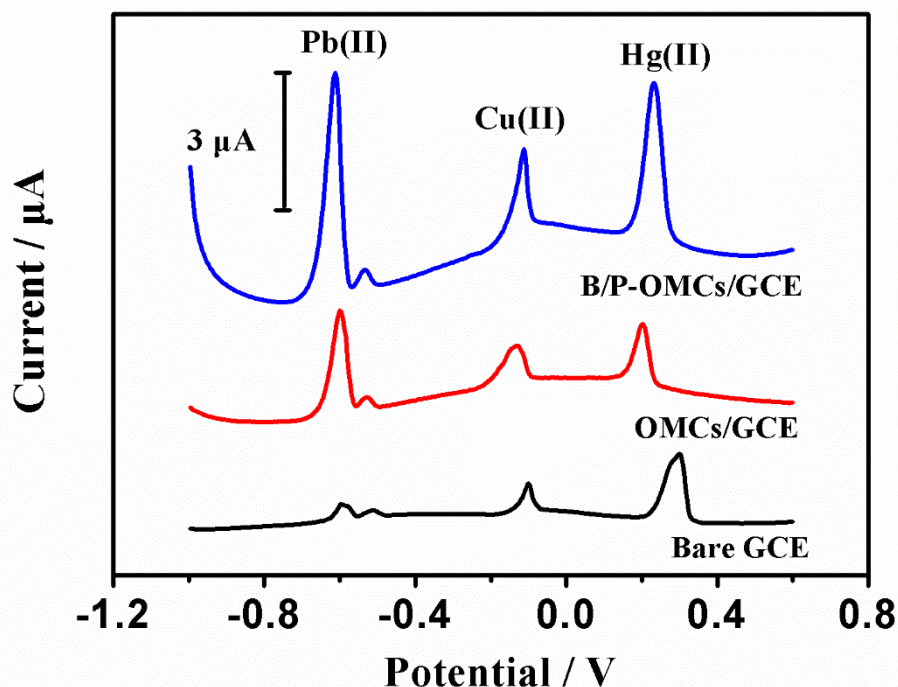
OMCs afford a better ordered mesostructure over a long-range. Raman spectrum is an effective method to describe the microstructure of materials. In order to study the graphitization degree of B/P-doped OMCs, Raman measurement was carried out, as shown in Fig. 2b. From the Raman spectrum, the sample shows two peaks at 1348 and 1591  $\text{cm}^{-1}$ , corresponding to D-band and G-band. In general, the D-band described as the defect degree in the graphite sheet, while the G-band is related to conjugated structure of  $\text{sp}^2$  hybrid [24]. The intensity ratio of  $I_D/I_G$  is usually used as an index of graphitization degree [25]. In our work, the  $I_D/I_G$  ratios of B/P-doped OMCs are 0.92, implying that the sample is higher graphitization degree, which is beneficial to improve its electrical conductivity and facilitate the electron transfer of materials.



**Figure 2.** (a) XRD patterns of B/P-doped OMCs, and OMCs, (b) Raman spectrum of B/P-doped OMCs sample.

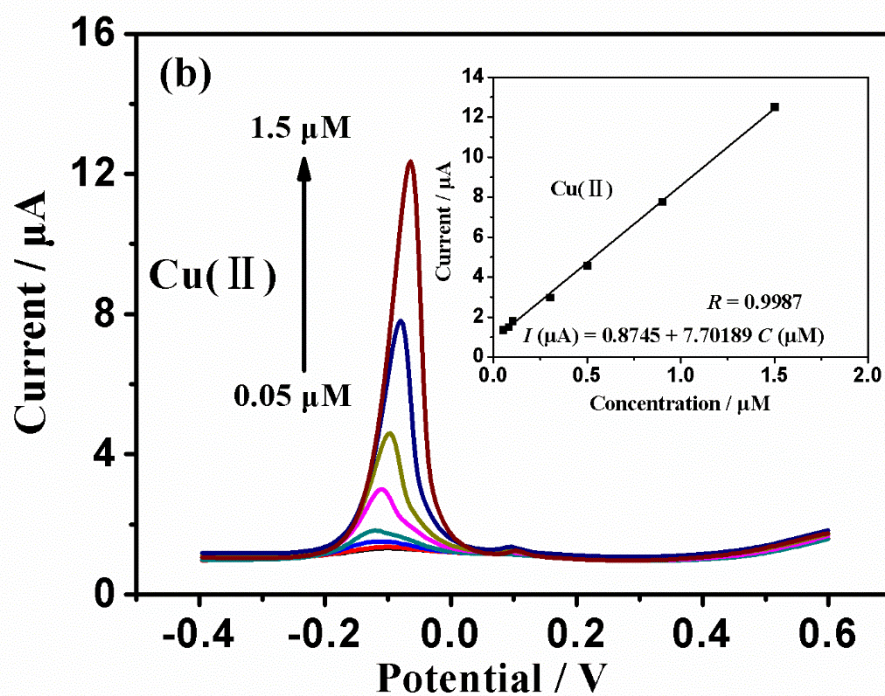
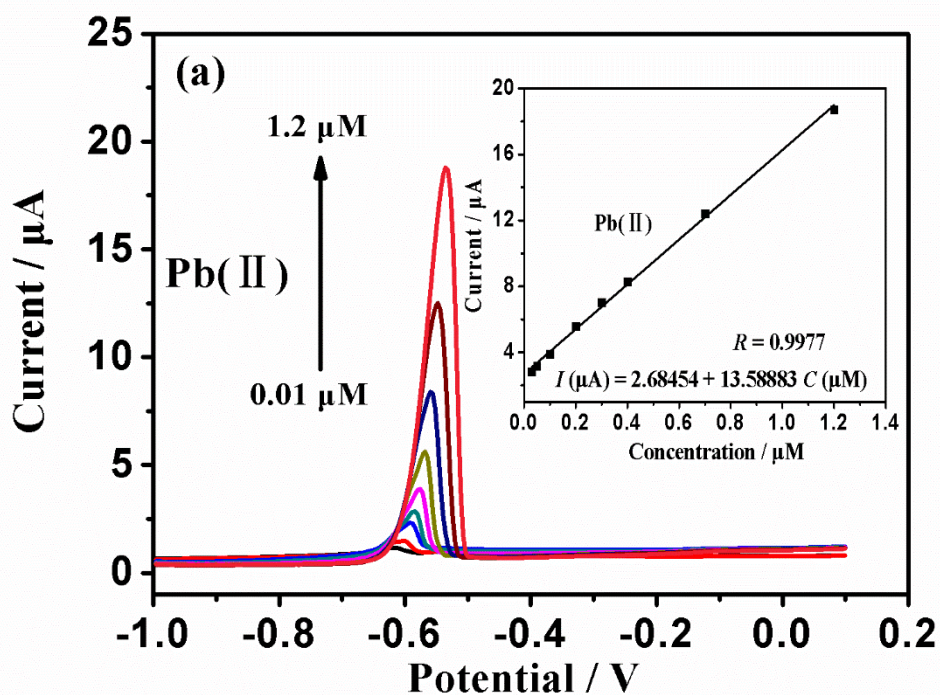
Fig. 3 displays the DPASV characteristics of bare, OMCs, and B/P-doped OMCs modified GCE. When the differential pulse anodic stripping voltammetric was carried out in a solution containing 0.5  $\mu\text{M}$  of  $\text{Pb}^{2+}$ ,  $\text{Cu}^{2+}$ , and  $\text{Hg}^{2+}$  in 0.1 M acetate buffer (pH 5.0), the responses at bare GCE were weak, and

also weak peaks at OMCs modified GCE were observed in the potential range of  $-1.0$  to  $+0.6$  V (vs. SCE). However, the sharper and higher peak current for the three target metal ions were obtained at the B/P-doped OMCs electrode.



**Figure 3.** DPASV for  $0.5 \mu\text{M}$  of Pb(II), Cu(II), and Hg(II) on bare, OMCS, and B/P-doped OMCs modified GCE in  $0.1 \text{ M}$  acetate buffer (pH 5.0), vs. SCE.

Under the optimal experimental conditions, Pb(II), Cu(II) and Hg(II) were examined simultaneously and individually at the B/P-modified electrode using DPASV. Fig. 4a showed the DPASV responses toward Pb(II) on a concentration range from  $0.01$  to  $1.2 \mu\text{M}$ . The general linear equation was  $I (\mu\text{A}) = 2.68454 + 13.58883 C (\mu\text{M})$ , and the correlation coefficient was up to  $0.9977$  (inset of Fig. 4a) and with the LOD of  $7.245 \times 10^{-10} \text{ M}$  ( $3\sigma$  method). Fig. 4b showed the DPASV responses of the B/P-doped OMCs electrode toward Cu(II) over a concentration range from  $0.05$  to  $1.5 \mu\text{M}$ . The linear equation of Cu(II) was  $I (\mu\text{A}) = 0.8745 + 7.70189 C (\mu\text{M})$ , and the correlation coefficient was up to  $0.9987$  (inset of Fig. 4b) and with the LOD of  $1.974 \times 10^{-9} \text{ M}$  ( $3\sigma$  method). Fig. 4c showed the DPASV responses of the B/P-doped OMCs electrode toward Hg(II) over a concentration range from  $0.001$  to  $0.1 \mu\text{M}$ . The linear equation of Hg(II) was  $I (\mu\text{A}) = 1.38526 + 65.87259 C (\mu\text{M})$ , and the correlation coefficient was up to  $0.9975$  (inset of Fig. 4c) and with the LOD of  $1.846 \times 10^{-10} \text{ M}$  ( $3\sigma$  method). Therefore, the B/P-doped OMCs electrode could play the role of a good platform for the determination of heavy metal ions.



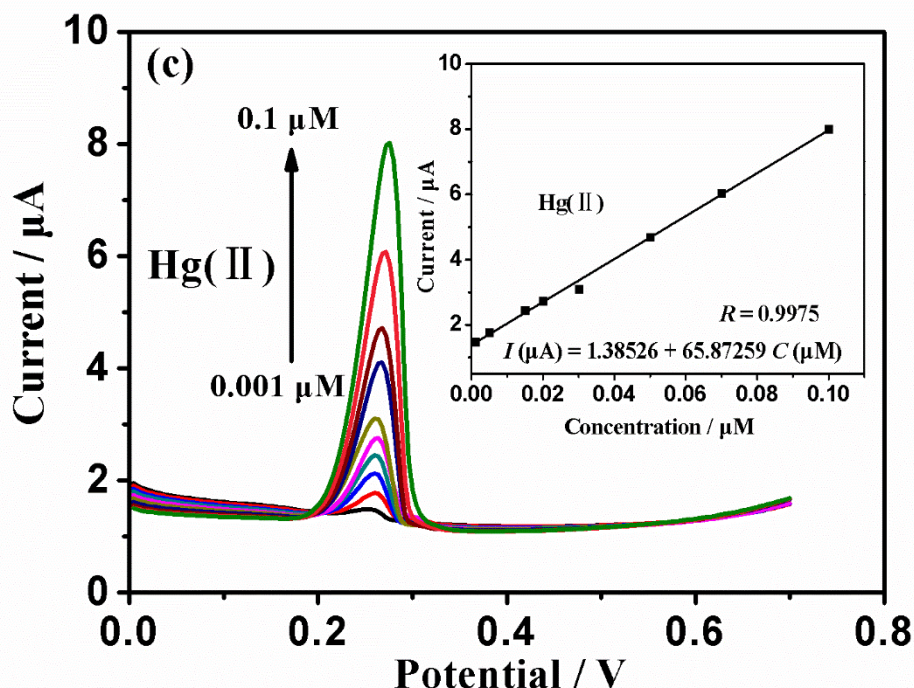


**Figure 4.** DPASV response of the B/P-doped OMCs modified GCE for the individual analysis of (a) Pb(II) over a concentration range from 0.01 to 1.2  $\mu\text{M}$ , (b) Cu(II) over a concentration range from 0.05 to 1.5  $\mu\text{M}$ , and (c) Hg(II) over a concentration range from 0.002 to 0.1  $\mu\text{M}$ .

The typical results of DPASV analysis by B/P-doped OMCs electrode for the simultaneous analysis of Pb(II), Cu(II), and Hg(II) with increasing concentrations under the optimized experimental conditions were shown in Fig. 5. The B/P-doped OMCs was successfully used to the simultaneous detection for the three target heavy metal ions of Pb(II), Cu(II), and Hg(II). It represented individual peaks in their coexistence at about  $-0.58$ ,  $-0.11$ , and  $0.28$  V vs. SCE for Pb(II), Cu(II), and Hg(II), respectively. The separation of the voltammetric peaks is large enough, therefore the simultaneous and selective detection using the B/P-doped OMCs electrode is practicable. The corresponding calibration curves were shown in Fig. 6a, and the Pb(II) was constructed from  $0.05 \mu\text{M}$  to  $0.5 \mu\text{M}$ . The linearization equation was  $I (\mu\text{A}) = 1.45428 + 5.87486 C (\mu\text{M})$ , and the corresponding correlation coefficient was up to 0.9981 (inset of Fig. 6a). The LOD of Pb(II) was calculated to be  $8.795 \times 10^{-9}$  M ( $3\sigma$  method). The corresponding calibration curves were shown in Fig. 6b, and the Cu(II) was constructed from  $0.05 \mu\text{M}$  to  $0.5 \mu\text{M}$ . The linear equation was  $I (\mu\text{A}) = 1.59309 + 3.98303 C (\mu\text{M})$ , and the corresponding correlation coefficient was up to 0.9980 (inset of Fig. 6b). The LOD of Cu(II) was calculated to be  $2.143 \times 10^{-9}$  M ( $3\sigma$  method). The corresponding calibration curves were shown in Fig. 6c, and the Hg(II) was constructed from  $0.05 \mu\text{M}$  up to  $0.5 \mu\text{M}$ . The linear equation was  $I (\mu\text{A}) = 1.02768 + 8.47698 C (\mu\text{M})$ , and the corresponding correlation coefficient was up to 0.9981 (inset of Fig. 6c). The LOD of Hg(II) was calculated to be  $1.385 \times 10^{-9}$  M ( $3\sigma$  method). These obtained LOD from our work were far more below the guideline value given by the World Health Organization (WHO).

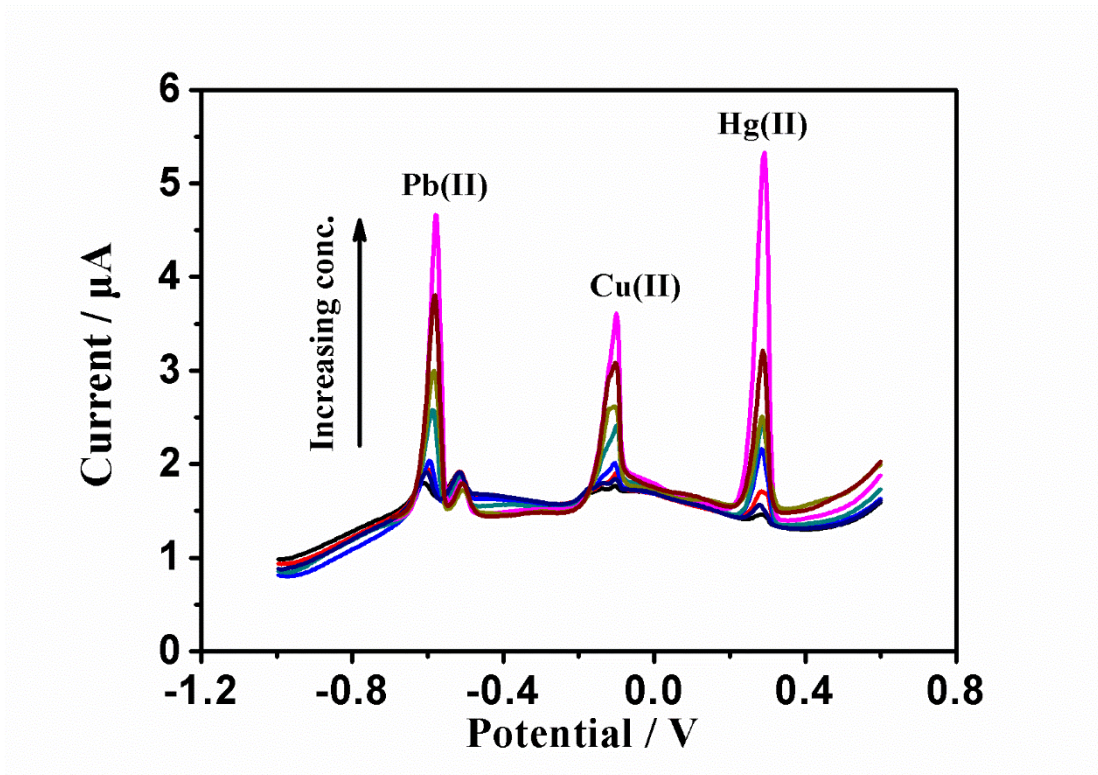
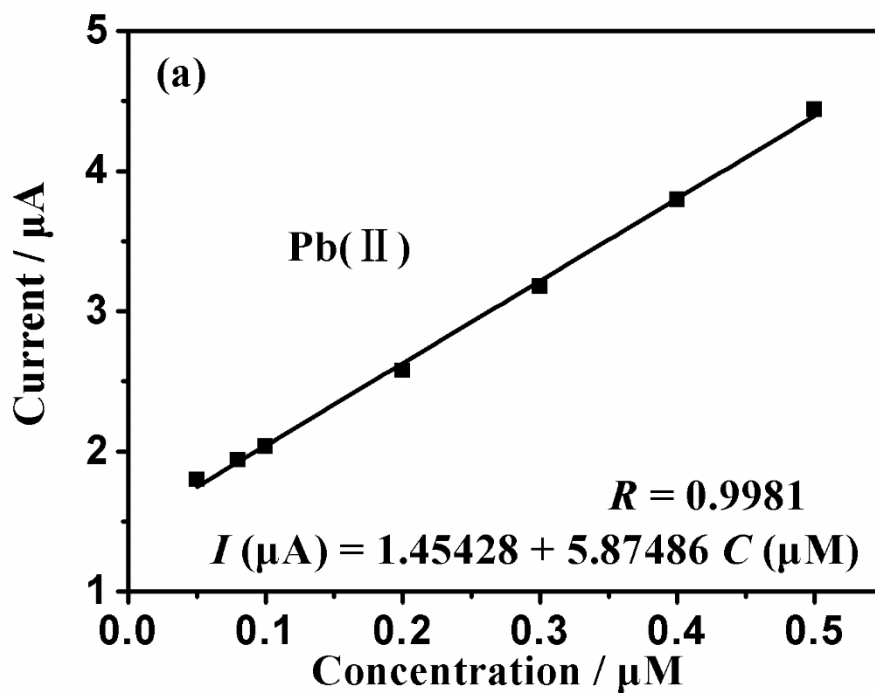


Figure 5. DPASV response of the B/P-doped OMCs for the simultaneous analysis of Pb(II), Cu(II), and Hg(II) over a concentration range from 0.05 to 0.5 μM for each metal ions, vs. SCE.



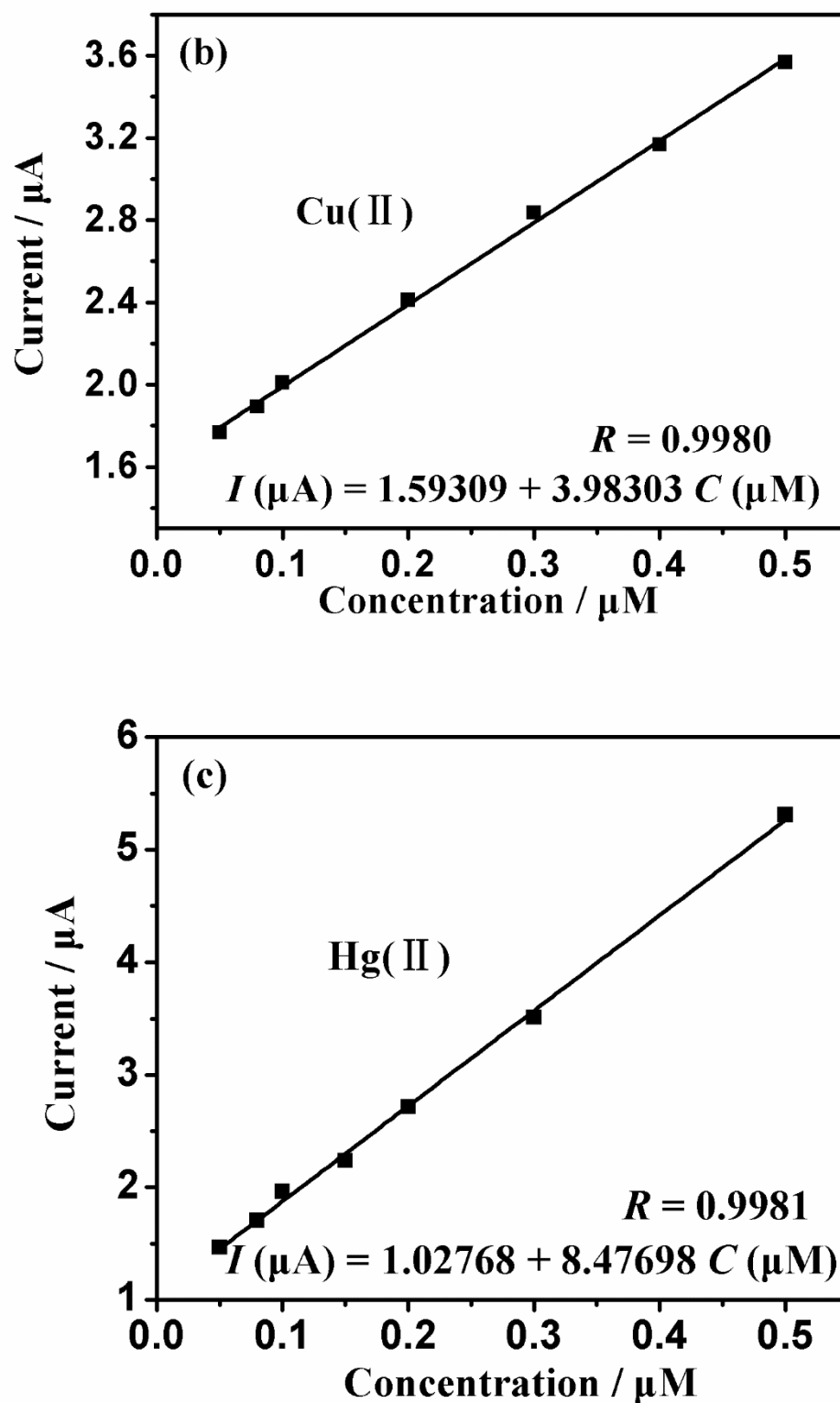
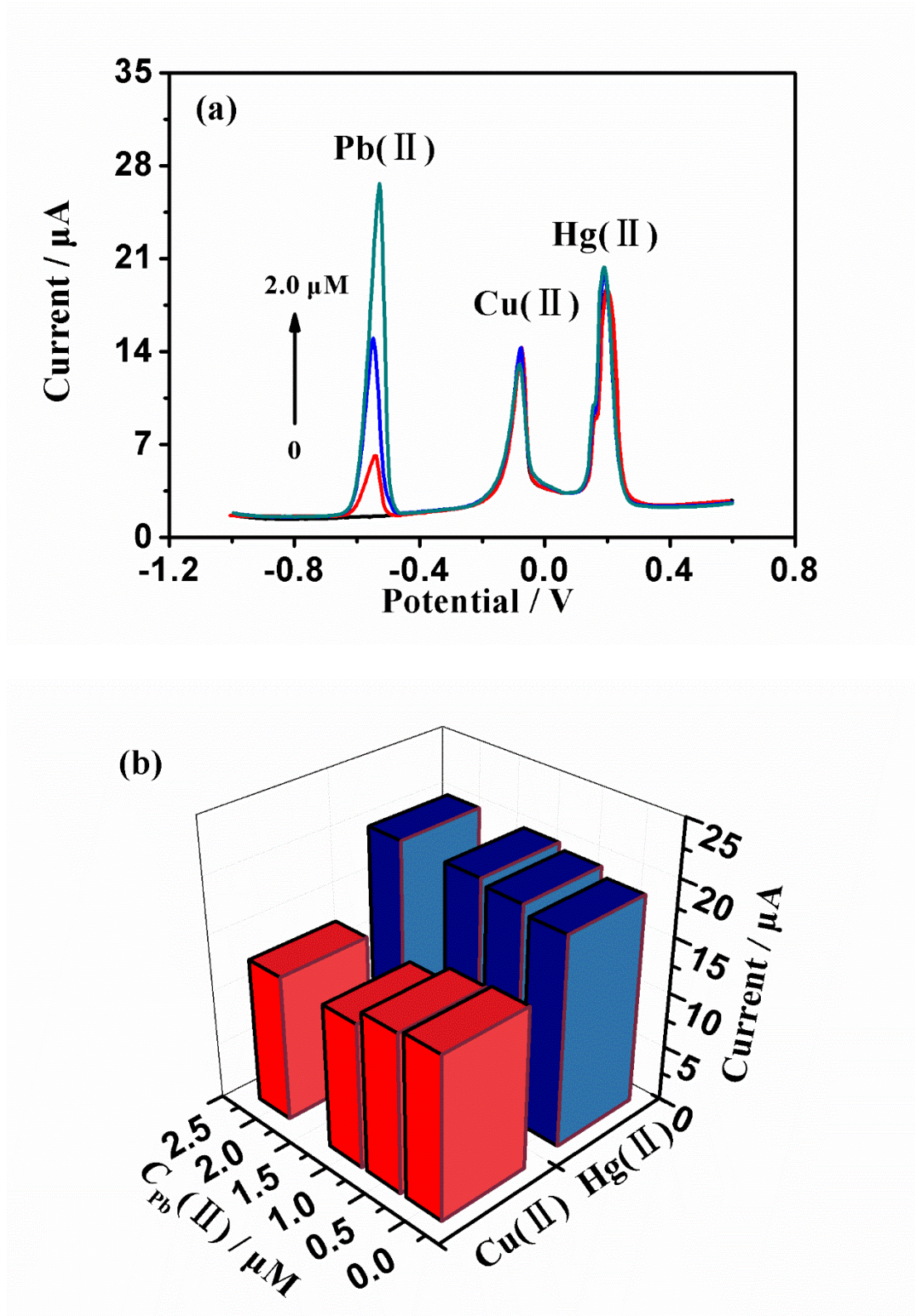


Figure 6. The respective calibration curves of Pb(II), Cu(II), and Hg(II) corresponding to Fig. 5.



**Figure 7.** (a) DPASV response of the B/P-doped OMCs electrode at 0, 0.5, 1.0, and 2.0  $\mu\text{M}$  Pb(II) in the presence of 1.5  $\mu\text{M}$  Hg(II) and Cu(II) in 0.1 M acetate buffer (pH 5.0), showing the interference of the concentrations of Pb(II) on the anodic peak currents of 1.5  $\mu\text{M}$  Hg(II) and Cu(II). (b) Comparison of the voltammetric peak current of Cu(II) and Hg(II) at different concentrations of Pb(II) corresponding to panel a.

Toward a better understanding of the enhancement in sensitivity, the DPASV responses of the B/P-doped OMCs electrode at different concentrations of Pb(II) in the presence of 1.5  $\mu\text{M}$  Cu(II) and Hg(II) was investigated (Fig. 7). It can be observed that in the Fig. 7 the peak currents of Cu(II) and Hg(II) increased slightly with the addition of Pb(II). Consequently, when the analysis was carried out at high level concentration of Pb(II), the significant increase of analytical signals were not observed.

**Table 1.** Comparison of the performance for determination of  $\text{Pb}^{2+}$ ,  $\text{Cu}^{2+}$ , and  $\text{Hg}^{2+}$  with others.

Electrodes	Method	Linear Ranges ( $\mu\text{M}$ )	LOD ( $\mu\text{M}$ )	Reference
F-GO/GCE	SWV	Cd(II), 1.0–6.0	/	[26]
		Pb(II), 1.0–6.0	/	
		Hg(II), 1.0–6.0	/	
		Cu(II), 1.0–6.0	/	
		Zn(II), not applicable	not applicable	
F-MWCNT/Fe <sub>3</sub> O <sub>4</sub> /0.5% Nafion/GCE	SWV	Cd(II), 0.048–30.0	0.014	[27]
		Pb(II), 0.028–30.0	0.0084	
		Hg(II), 0.013–32.5	0.0039	
		Cu(II), 0.017–31.5	0.0053	
		Zn(II), 0.039–32.5	0.012	
Ag-bipy-CP/PMB/GCE	DPV	Pb(II), 0.02–0.1	0.01	[28]
		Hg(II), 0.001–0.05	0.0005	
		Cu(II), 0.02–0.1	0.01	
BTPSBA/CPE	DPASV	Pb(II), 0.3–7	0.04	[29]
		Hg(II), 2–10	0.4	
		Cu(II), 0.8–10	0.2	
L-cys-rGO/GCE	DPASV	Cd(II), 0.4–2	0.03	[30]
		Pb(II), 0.4–1.2	0.02	
		Hg(II), 0.4–2	0.01	
(G)-MWCNTs/CPE	ASV	Cu(II), 0.4–2	0.04	[31]
		Cd(II), 0.05–0.028	0.001	
		Pb(II), 0.02–0.14	0.001	
Nafion-G/GCE	ASV	Cd(II), 0.01–0.28	0.0002	[32]
		Pb(II), 0.002–0.24	0.0001	
B/P-OMCs/GCE	DPASV	Pb(II), 0.01–1.2	0.007	This work
		Hg(II), 0.001–0.1	0.002	
		Cu(II), 0.05–1.5	0.02	

The comparison of B/P-doped OMCs/GCE with other modified electrodes for heavy metal ions electrochemical detection was listed in Table 1 [26-32]. The B/P-doped OMCs/GCE exhibited here can simultaneously supply analysis for three target heavy metal ions of  $\text{Pb}^{2+}$ ,  $\text{Cu}^{2+}$ , and  $\text{Hg}^{2+}$ . By investigating the influence of test conditions to optimize the electrochemical determination, we can simultaneously detect  $\text{Pb}^{2+}$ ,  $\text{Cu}^{2+}$ , and  $\text{Hg}^{2+}$  at a low concentration level in the experiments. Moreover, the sensing performance is good enough for implication in practice.

#### 4. CONCLUSIONS

A novel B/P-doped OMCs has been successfully synthesised. The B/P-doped OMCs can be applied in the modified electrodes for the simultaneous detection of Pb(II), Cu(II), and Hg(II). The obtained results suggest that B/P-doped OMCs is a promising material, which possesses the advantages of in electrochemical detection of heavy metal ions. The B/P-doped OMCs, has proved to be a sensitive electrode for Pb(II), Cu(II), and Hg(II) analysis using DPASV. The results of LOD were far more below the guideline value which given by the World Health Organization (WHO). The B/P-doped OMCs, have been proved to be a effective and sensitive for simultaneous detection of Pb(II), Cu(II), and Hg(II) in aqueous solutions or waste water using DPASV.

#### ACKNOWLEDGEMENTS

Financial support from the Research Program of Application Foundation of Qinghai Province (No. 2019-ZJ-7013), Innovation ability improvement program of colleges and Universities of Gansu province (No.2020B-233) and Teacher Doctoral Research Start-Up Funding of Lanzhou City University (LZCU-BS2015-09).

#### References

1. X. Song, R. Wang, W. Zhao, S. Sun and C. Zhao, *J. Colloid Interf. Sci.*, 485 (2017) 39–50.
2. C.S. Cheng, J. Deng, B. Lei, A. He, X. Zhang, L. Ma, S. Li and C. Zhao, *J. Hazard. Mater.*, 263 (2013) 467–478.
3. G. Chen, C. Qiao, Y. Wang and J. Yao, *Ind. Eng. Chem. Res.*, 53 (2014) 15576–15581.
4. Z.L. Wu, F. Liu, C.K. Li, X.Q. Chen and J.G. Yu, *Colloids Surf. A: Physicochem. Eng. Asp.*, 509 (2016) 65–72.
5. H.W. Liang, X. Cao, W.J. Zhang, H.T. Lin, F. Zhou, L.F. Chen and S.H. Yu, *Adv. Funct. Mater.*, 21 (2011) 3851–3858.
6. E.M. Faouzi, N. Bensalah and A. Gadri, *J. Hazard. Mater.*, 168 (2009) 1163–1169.
7. R. Fang, X. Cheng and X. Xu, *Bioresour. Technol.*, 101 (2010) 7323–7329.
8. G. Liu, T. Wu, J. Zhao, H. Hidaka and N. Serpone, *Environ. Sci. Technol.*, 33 (1999) 761–766.
9. S.M.D.A.G. Ulson, K.A.S. Bonilla and A.A.U. de Souza, *J. Hazard. Mat.*, 179 (2010) 35–42.
10. Q. Liu, Q. Liu, Z. Wu, Y. Wu, T. Gao and J. Yao, *Acs Sustain. Chem. Eng.*, 5 (2017) 1871–1880.
11. G.P. Rao, C. Lu and F.S. Su, *Sep. Purif. Technol.*, 58 (2007) 224–231.
12. J. Lee, J. Kim and T. Hyeon, *Adv. Mater.*, 18 (2006) 2073–2094.
13. C.D. Liang, Z.J. Li and S. Dai, *Angew. Chem., Int. Ed.*, 47 (2008) 3696–3717.
14. Y.F. Shi, Y. Wan and D.Y. Zhao, *Chem. Soc. Rev.*, 40 (2011) 3854–3878.
15. D.S. Su, J. Zhang, B. Frank, A. Thomas, X.C. Wang, J. Paraknowitsch and R. Schlogl, *ChemSusChem*, 3 (2010) 169–180.
16. J.M. Carlsson and M. Scheffler, *Phys. Rev. Lett.*, 96 (2006) 046806.
17. X. Jin, V.V. Balasubramanian, S.T. Selvan, D.P. Sawant, M.A. Chari, G.Q. Lu and A. Vinu, *Angew. Chem. Int. Ed.*, 48 (2009) 7884–7887.
18. A.H. Lu, J.J. Nitz, M. Comotti, C. Weidenthaler, K. Schlichte, C.W. Lehmann, O. Terasaki and F. Schuth, *J. Am. Chem. Soc.*, 132 (2010) 14152–14162.
19. Y.J. Zhang, T. Mori, J.H. Ye and M. Antonietti, *J. Am. Chem. Soc.*, 132 (2010) 6294–6295.
20. E. Frackowiak and F. Beguin, *Carbon*, 39 (2001) 937–950.

21. L.L. Zhang and X.S. Zhao, *Chem. Soc. Rev.*, 38 (2009) 2520–2531.
22. D.S. Su and R. Schlogl, *ChemSusChem*, 3 (2010) 136–168.
23. E. Raymundo-Pinero, M. Cadek, M. Wachtler and F. Beguin, *ChemSusChem*, 4 (2011) 943–949.
24. M. Wu, Y. Li, B. Yao, J. Chen, C. Li and G. Shi, *J. Mater. Chem. A*, 4 (2016) 16213–16218.
25. X.T. Xu, H.M. Tang, M. Wang, Y. Liu, Y.J. Li, T. Lu and L.K. Pan, *J. Mater. Chem. A*, 4 (2016) 16094–16100.
26. A.R. Thirupathi, B. Sidhureddy, W. Keeler and A.C. Chen, *Electrochem. Commun.*, 76 (2017) 42–46.
27. W. Wu, M. Jia, Z. Wang, W. Zhang, Q. Zhang, G. Liu, Z. Zhang and P. Li, *Microchim. Acta*, 186 (2019) 1–10.
28. A. Chira, B. Bucur, M.P. Bucur and G.L. Radu, *New J. Chem.*, 38 (2014) 5641–5646.
29. I. Cesarino, G. Marino, J.R. Matos, E.T.G. Cavalheiro and I. Cesarinoetal, *Talanta*, 75 (2008) 15–21.
30. S. Muralikrishna, K. Sureshkumar, Thomas S. Varley, D.H. Nagaraju and T. Ramakrishnappa, *Anal. Methods*, 6 (2014) 8698–8705.
31. H. Huang, T. Chen, X.Y. Liu and H.Y. Ma, *Anal. Chim. Acta*, 852 (2014) 45–54.
32. J. Li, S.J. Guo, Y.M. Zhai and E.K. Wang, *Anal. Chim. Acta*, 649 (2009) 196–201.

© 2020 The Authors. Published by ESG ([www.electrochemsci.org](http://www.electrochemsci.org)). This article is an open access article distributed under the terms and conditions of the Creative Commons Attribution license (<http://creativecommons.org/licenses/by/4.0/>).